Desalination and Water Treatment
www.deswater.com

35 (2011) 195–201
November

doi: 10/5004/dwt.2011.2485

Dairy wastewater purification by vibratory shear enhanced processing

Szabolcs Kertész, Zsuzsanna László*, Endre Forgács, Gábor Szabó, Cecilia Hodúr

Faculty of Engineering, Department of Process Engineering, University of Szeged, Moszkvai krt 5–7, Szeged, H-6725, Hungary
Tel. +3654626526; Fax: +3665626549; email: zsizsu@chem.u-szeged.hu

Received 15 November 2010; Accepted 23 May 2011

ABSTRACT

This study investigated the performance of a Vibratory Shear Enhanced Processing (VSEP) using ultrafiltration (UF), nanofiltration (NF) and reverse osmosis (RO) membrane system for decreasing of chemical oxygen demand (COD) from dairy wastewater. Three commercially available membranes having different pore sizes were used to compare their relative efficiency for COD decreasing. Permeate flux and membrane rejection of COD were measured as well as mean shear rates and the specific energy demands of vibrated and non-vibrated methods were calculated and compared. Furthermore, flux and COD rejection were also studied increasing by transmembrane pressure (TMP) and vibration amplitude. Concentration test were performed by UF, NF and RO.

Keywords: VSEP; Dairy wastewater; Shear rate; Amplitude; Energy consumption; Vibration

1. Introduction

Large amount of wastewater produced form diverse industrial sources needs to be treated before the sewage system. The dairy industry generates large amount of effluents containing lactose, protein, ionic content and fat (in smaller amount). Membrane separation is one of the effective technologies to treat dairy wastewaters [1].

The effectiveness and success of membrane separation processes is decreased by fouling [2]. One possible method to decrease the fouling rate is to increase the liquid shear rate next to the surface of the membrane, other methods include altering the feed liquid flow. To change flow geometry by a turbulence-promoting spacer or static mixer [3,4].

The concentration polarization (what is responsible for the polarization layer formation on the surface of the membrane, liable for polarization layer resistance) is caused by accumulation of substances on the membrane surface. Inner pores fouling (liable for fouling resistance) is caused by the particles, which could be going into the membrane pores and to attach on the inner wall of the pores. Several methods have been developed in various applications of membrane processes to reduce concentration polarization and membrane fouling, such as flocculation, high-shear rotary membranes or chemical cleaning [5,6].

VSEP technology has been successfully used to treat wastewaters, including dairy, livestock, pulping wastewaters and pig manure [7–11].

By using a vibrating membrane filtration system in these studies, vibration of the membrane prevented surface fouling or at least greatly reduced the extent of fouling, resulting in higher permeate fluxes and longer operating times.

These studies have used the full range of available membranes and have demonstrated significant advantages of the VSEP system over conventional membrane processes.

The conventional membrane process, especially the NF and RO, needs high TMP to ensure the continuous

*Corresponding author.

PERMEA 2010 – Membrane Science and Technology Conference of Visegrád Countries (Czech Republic, Hungary, Poland, Slovakia), September 4–8, 2010, Tatranské Matliare, Slovakia

flow throughout the membrane, thus these processes may be relatively expensive mainly because of the high energy demand of the pump. The VSEP system permits high shear rates on the membrane surface by the inertia of the fluid motion and not only by the feed flow, which can be set very low.

Earlier studies investigated dairy wastewaters treatments by VSEP were performed in model solutions, mainly in diluted milk solutions [7].

The aim of this study was to investigate the effect of vibration during UF, NF and RO of real dairy wastewater. The energy demand of VSEP (including vibrational energy demand and energy consumption of the pump) also was compared to the non-vibrated method.

2. Materials and methods

2.1. Feed solution

The dairy wastewater was provided by Alföldi Garabonciás Kft. (Izsák, Hungary). The main characteristics of the raw feed wastewater are given by Table 1.

2.2. Membrane filtration

The filtration module was an L-mode VSEP (New Logic International, Emeryville, CA, USA) equipped with an annular single membrane (with an effective area of 503 cm^2), separated from the permeate by a support screen and a drainage cloth. The membrane was enclosed in the membrane chamber/module, which was supported by a central shaft. The module was placed at the tip of a 1.5 m vertical shaft. This shaft acts as a torsion spring, which transmits the vibrations created by an eccentric drive motor. The membrane vibrates azimuthally in its own plane with amplitude depending upon frequency (F) and the membrane rotates a short distance in one direction and then reverses itself. Due to this vibrations, the local membrane shear rate varies sinusoidally with time and proportionally to the radius. The resulting motion of the housing was indicated by the manufacturer to be 32 mm on the outer rim at the maximum frequency allowed of 60.75 Hz.

The measurements were carried out at 50°C in all cases. Generally TMP was set to 0.8 MPa, 2 MPa and 3 MPa during UF, NF and RO respectively at 50 ± 1°C and the amplitude of the vibration was set to 25.4 mm (1 inch) and frequency to 54.8 Hz. The wastewater from the tank was pumped to the inlet of the VSEP system.

2.3. Membrane conditioning and cleaning

The flat-sheet membranes (7 kDa PES5 polyethersulfone for UF, 240 Da NF-270 TFC polyamide for NF and 50 Da BW-30 polyamide for RO) were submerged in deionized water overnight. Before the measurements, the membranes were treated by circulating deionized water at low pressure at a high recirculation flow rate for 1 h in order to remove the excess of preservation chemicals attached to the new membranes. After these conditioning steps, deionized water was permeated at same pressures as in the concentration processes (at 0.8 MPa, 2 MPa and 3 MPa during UF, NF and RO respectively), in order to measure the corresponding water permeation fluxes (J_W) and to establish the hydraulic permeability of the clean membrane. Membrane application in dairy industries is faced with the important issue of membrane fouling by certain whey components, mainly proteins. Furthermore, membrane cleaning is an important economic process. In our case, the procedure for membrane cleaning was as following: (1) a rinsing step with deionized water, (2) exposure to pepsin enzyme solution (1 w/w%) for 30 min at 40°C, (3) a cleaning procedure with an alkaline (SDS, NaOH and EDTA) 0.5 w/w% solution for 30 min at 50°C, and (4) a final rinse with deionized water [12]. The cleaning procedures were repeated until at least 90% of the initial J_W was recovered.

2.4. Analytical methods

The COD was determined in test tubes with an ET 108 digester and a PC CheckIt photometer (Lovibond, Germany). The turbidity of the permeate and concentrate was determined with a HACH2100AN turbidimeter (Hach, Germany). During the VSEP process, the maximum ($\gamma_{w,\max}$) and mean ($\bar{\gamma}_w$) shear rates at the membrane surface were calculated via the following equations [13]:

$$\gamma_{w,\max} = \sqrt{2}d(\pi F)^{3/2}\ v^{-1/2} \qquad [s^{-1}], \tag{1}$$

$$\bar{\gamma}_\omega = \frac{2^{3/2}(R_2^3 - R_1^3)}{3\pi R_2(R_2^2 - R_1^2)}\gamma_{w,\max} \qquad [s^{-1}] \tag{2}$$

Table 1
Dairy wastewater parameters at 50°C

	Conductivity [mS cm^{-1}]	TSS [°Brix]	Turbidity [NTU]	COD [mg/l]	Viscosity [mPas]	Density [g/cm^3]	pH [-]
Dairy wastewater	2.7	1.1	2170	8175	0.999	0.9988	4.62

where d is the peak to peak vibration amplitude at the periphery of the membrane [m], F is the vibration frequency [s^{-1}], and ν is the kinematic viscosity of the fluid [m^2s^{-1}]. R_2 is the inner radius (0.047 m) and R_1 is the outer radius (0.135 m) of the circular membrane module housing.

The flux was determined via the equation:

$$J = \frac{dV}{dt}\frac{1}{A} \qquad [\mathrm{Lm^{-2}h^{-1}}] \tag{3}$$

From the values of flux the equivalent or normalised permeability ($J_{norm.}$) (referring to unit surface (A) [m^2], unit pressure difference (Δp) [MPa], unit time (t) [s]) were determined via the following formula:

$$J_{\mathrm{norm.}} = \frac{J}{\Delta p} \qquad [\mathrm{Lm^{-2}h^{-1}MPa^{-1}}] \tag{4}$$

As the filtration process continues, fouling will eventually occur. This causes the permeate flux to decay with time. The decaying permeate flux is described by the power law:

$$J = J_0 \cdot t^{-k} \qquad [\mathrm{Lm^{-2}h^{-1}}] \tag{5}$$

where t is time [s], J_0 is the initial flux [$Lm^{-2}h^{-1}$] and k is the fouling rate constant [-]. Both J_0 and k can be calculated from the measured data by using the curve-fitting technique.

In order to investigate the membrane fouling, the different fouling resistances were calculated. The rate and extent of membrane fouling and its effect on flux for any given systems depend on various parameters, such as the specific interactions between the membrane surface and various fouling species, hydrodynamic forces exerted by the flowing process fluid and process parameters such as the cross-flow velocity, TMP, feed concentration, pore size and temperature.

$$J_W = \frac{\Delta p}{\eta_W R_M} \qquad [\mathrm{Lm^{-2}h^{-1}}] \tag{6}$$

where J_W is the water flux of the clean membrane, η_W is the water viscosity [Pas], Δp is the pressure difference between the two sides of the membrane [MPa] and R_M is the membrane resistance.

R_T is the total resistance [m^{-1}], can be evaluated from the steady-state flux by using the resistance-in-series model:

$$R_T = R_M + R_F + R_P \qquad [\mathrm{m^{-1}}] \tag{7}$$

where R_F is the fouling resistance (mainly by the fouled pores) [m^{-1}] and R_P is the polarization layer resistance [m^{-1}].

The membrane resistance was calculated as

$$R_M = \frac{\Delta p}{J_W \eta_W} \qquad [\mathrm{m^{-1}}] \tag{8}$$

The resistance of the polarization layer was determined after rinsing with deionized water to remove any particles residue layer from the surface of the membrane [13], by subtracting the resistance of the clean membrane:

$$R_F = \frac{\Delta p}{J_{WA}\eta_W} - R_M \qquad [\mathrm{m^{-1}}], \tag{9}$$

$$R_P = \frac{\Delta p}{J_C \eta_{WW}} - R_M - R_F \qquad [\mathrm{m^{-1}}], \tag{10}$$

where J_{WA} is the water flux after concentration tests, J_C is the constant flux at the end of the concentration and η_{WW} is the wastewater viscosity.

The selectivity of a membrane for a given solute was expressed by the average rejection (R)

$$R = \left(1 - \frac{c}{c_0}\right)100 \qquad [\%] \tag{11}$$

where c is the average concentration of the solute in the permeate phase, and c_0 is the concentration of the solute in the feed.

The specific energy demands (e) of membrane processes were calculated by means of the following equations:

$$e_v = \frac{P_{VM} \cdot \eta_{VM} + P_{FP} \cdot \eta_{FP}}{A \cdot J} \qquad [\mathrm{kWhm^{-3}}], \tag{12}$$

$$e_{NV} = \frac{P_{FP} \cdot \eta_{FP}}{A \cdot J} \qquad [\mathrm{kWhm^{-3}}], \tag{13}$$

where e_V is the vibration specific energy demand and e_{NV} is the non-vibration specific energy demand, P_{VM} is the power consumption of the vibrational motor [kWh], P_{FP} is the power consumption of the feed pump [kWh], η_{VM} is the efficiency of the vibrational motor, η_{FP} is the efficiency of the feed pump, A is the area of the membrane filter (503 cm^2) and J is the flux [$m^3m^{-2}h^{-1}$].

3. Results

3.1. The effect of vibration on permeate flux and membrane resistance

The variations of permeate fluxes in the function of the filtration time are illustrated in Fig. 1. The vibration amplitude was set to 24.5 mm in order to ensure the possibly highest shear rates at the membrane surface.

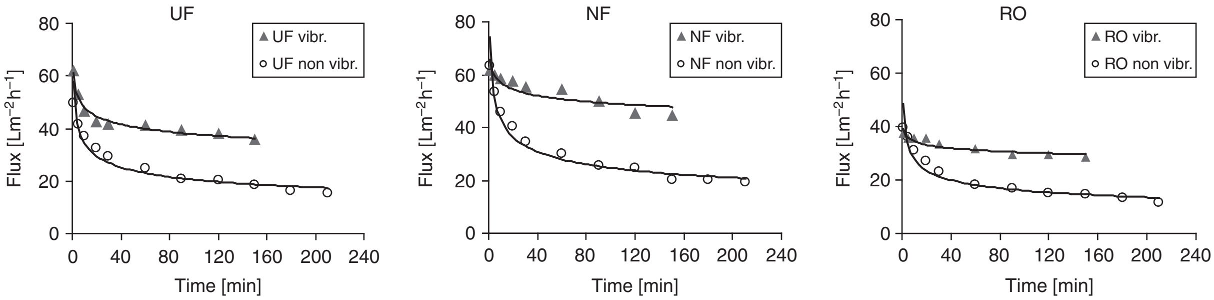

Fig. 1. Permeate flux vs. time during UF, NF and RO without and with membrane vibration.

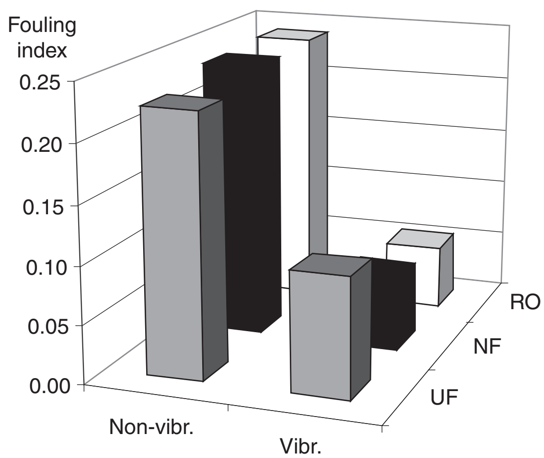

Fig. 2. Comparison of fouling indexes.

It was found that the membrane vibration increased the permeate flux in all cases. The flux increasing was most obvious during NF (almost 3 times higher fluxes were obtained using vibration) but 2 times higher permeate flux was achieved during UF and RO.

It was found that obtained experimental data fitted well the power law model (Eq. 5). This model was used to calculate and compare the *k* fouling indexes.

The Fig. 2. shows that the fouling indexes were decreased by using vibration, which means that the initial high permeate flux does not decrease so fast than without vibration. The most dramatical decreasing was observed during NF and RO.

In order to investigate the membrane fouling, the different fouling resistances were calculated using Eqs. (6–10).

It was found that – as it was expected – the total membrane resistance increased with decreasing membrane pore diameter, it is the highest during RO (Fig. 3). The vibration decreased the membrane resistances, both fouling and polarization layer resistance, according to the results of calculation fouling index. Similar results have been found earlier during UF of natural organic matter (NOM) by VSEP system [14].

According to the results of fouling index calculations, the decreasing of the total resistances also was observed. On the other hand, the composition of the total resistance mightily changed: the polarization layer resistance decreased remarkably and the fouling resistance decreased through vibration.

Since the UF membranes have higher pore size than NF or RO, the molecules, which are caught into the membrane porous, can release easier during the vibration. Hence, the fouling resistance during UF operation will decrease to a larger extent.

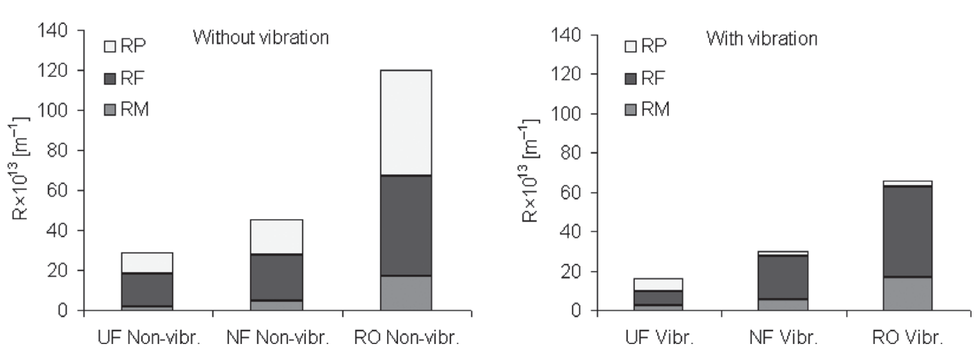

Fig. 3. The content of total membrane resistances without and using vibration during UF, NF and RO.

Since the salt content of the feed was relatively high, the osmotic pressure difference between the retentate and permeate side of the membrane also affects on the net driving force, thus a portion of the total resistance is contributed by difference in salt concentrartion between two sides of the membrane (mainly in the case of NF and RO). In our case the effect of the salt concentration is appeared as a part of polarisation layer resistance contributed to concentration polarisation.

3.2. Effect of vibration amplitude

In order to evaluate the effect of vibration amplitude on the membrane separation process, the filtration was performed with different vibration amplitudes, by applying TMP 0.8, 2 and 3 MPa during UF, NF and RO respectively. The fluxes versus vibration amplitudes are presented in Fig. 4.

The shear rate on the surface of the membrane is caused not only by vibration, but by the cross-flow velocity too. The differences of normalised flux ($\Delta J_{\text{norm.}}$) were expressed by the following equation:

$$\Delta J_{\text{norm.}} = J_{\text{norm.}V} - J_{\text{norm.}NV} \qquad [\text{Lm}^{-2}\text{h}^{-1}\text{MPa}^{-1}] \qquad (14)$$

where $J_{\text{norm.}V}$ is the normalised flux of vibrated solutions and $J_{\text{norm.}NV}$ is the normalised flux of non-vibrated solutions.

In Fig. 5. the $\Delta J_{\text{norm.}}/J_W$ flux differences were shown in the function of mean shear rates. The permeability increased with increasing shear rate in all cases. It was found that the vibration increases the flux most dramatically in the case of NF, than RO and UF. This can be explained by the difference in the structure and composition (e.g., salt content) of the polarization layer. In the case of NF and RO the composition of the polarization layer is very different resulting in different behaviour in the function of shear rate. In the case of UF the vibration decreased the porous fouling, but the decrease of the polarization layer was not so perceptible resulting minor flux increasing with shear rate.

3.3. Effect of vibration on COD rejection

Effect of vibration on elimination of the COD from dairy wastewater by UF, NF and RO also was examined. These experiments were performed applying TMP 0.8, 2 and 3 MPa during UF, NF and RO respectively, with 24.5 mm vibration amplitude at 50°C.

It was found that the vibration significantly increased the COD rejection during UF from 27.8% to 40.0%. Less increasing rejection was observed in the case of NF (90.5% from 87.4%) and RO (98.6% from 98.4%), but in these cases the rejection was high without vibration too; as it can be seen in Fig. 6, the vibration amplitude has no significant effect on rejection.

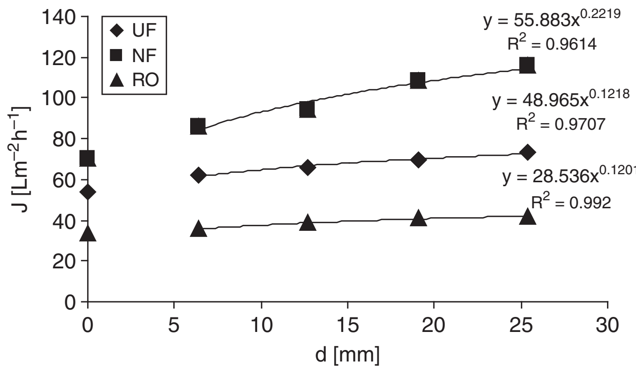

Fig. 4. Flux in relation to vibration amplitude during UF, NF and RO.

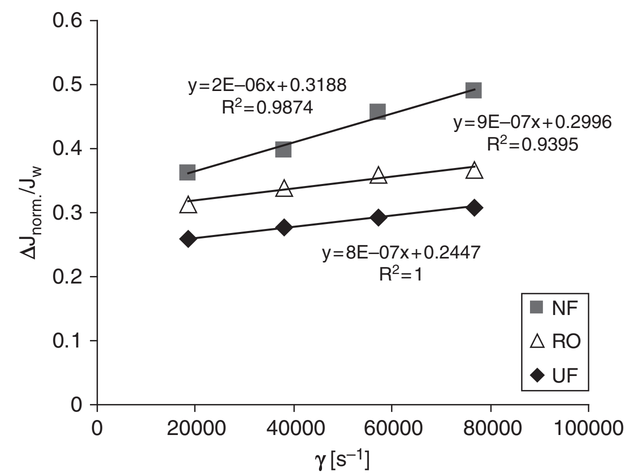

Fig. 5. Increment in the flux differences in relation to mean shear rate during vibration UF, NF and RO.

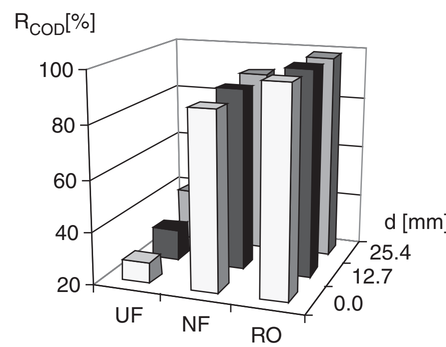

	UF	NF	RO
□ 0.00	27.79	87.39	98.41
■ 12.70	32.18	89.41	98.68
■ 25.40	39.87	90.53	98.64

Fig. 6. The effect of vibration amplitude on COD rejection during UF, NF and RO.

3.4. The specific energy demand of membrane filtration processes with and without vibration

The energy consumption of feed pump and vibratory system were measured, and the specific energy demand of membrane processes was calculated by means of the Eq. (12).

It was found that the power consumption of vibration was increased with vibration amplitude, while the consumption of feed pump was independent of amplitude. The main part of the total consumption was the feed pump demand. Calculating the powers per volume [m^3] of permeate, it was found that the vibration amplitude did not affect the specific energy demand (Fig. 7).

In the next series of experiments, the effect of TMP on specific energy demand was investigated in vibrating and non-vibrating membrane filtration systems. It was found that at maximized vibration amplitude the specific energy demand of UF and NF increased with TMP, while this was not so characteristic in the case of RO (Fig. 8). The specific energy demand became independent of TMP using vibratory module. It is important to note that during UF and NF at lower pressures the energy consumption of vibratory systems is higher than without vibration; but over a pressure limit the vibration become more economical. This type of pressure limit was not observed during RO; the energy demand of vibration systems was higher at all TMP.

The energy demand during concentration experiments was also measured. The results are shown in Fig. 9. It was found that at the beginning of the filtration (before the building of polarization layer on the surface of the membrane) the specific energy demand per m^3 permeate was lower at non-vibrating systems, but at the end of the concentration the vibration decreased the normalized specific energy demand. The difference between the vibrating and non-vibrating methods was most expressed in the case of RO, and there was only a slight difference in the case of UF.

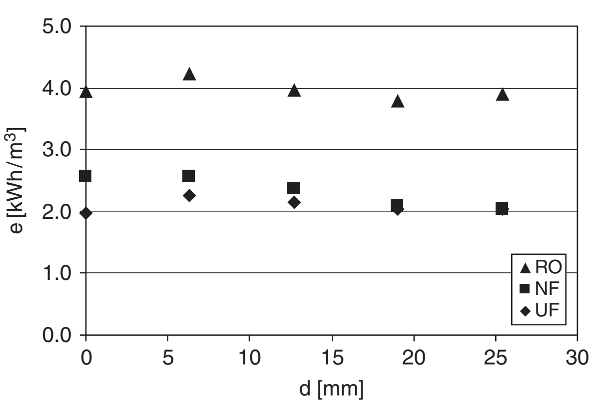

Fig. 7. The specific energy demand of the feed pump and vibratory module in the function of vibration amplitude.

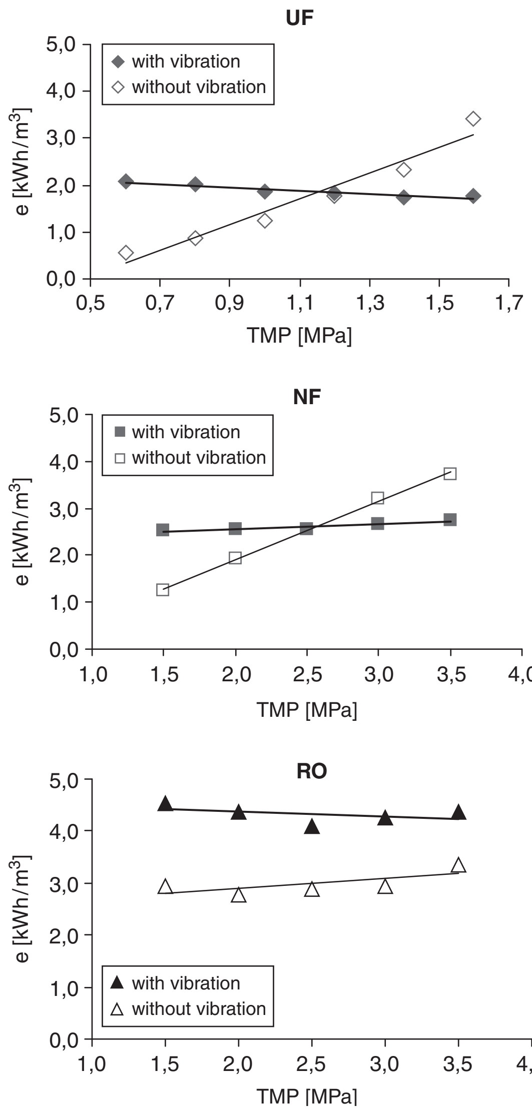

Fig. 8. Specific energy demand per m^3 permeate with and without vibration during UF, NF and RO.

4. Summary

This study investigated the performance of a Vibratory Shear Enhanced Processing (VSEP) using ultrafiltration (UF), nanofiltration (NF) and reverse osmosis (RO) membrane system for the decreasing of chemical oxygen demand (COD) from dairy wastewater. Three commercially available membranes (7 kDa PES5 (polyethersulfone) for ultrafiltration, 240 Da NF-270 TFC polyamide for nanofiltration and 50 Da BW-30 polyamide for reverse osmosis) having different pore sizes were used.

The results showed that the vibration mightily decreased the polarization layer on the surface of the membranes, decreasing the fouling resistances too. The permeability increases with increasing shear rate in all cases.

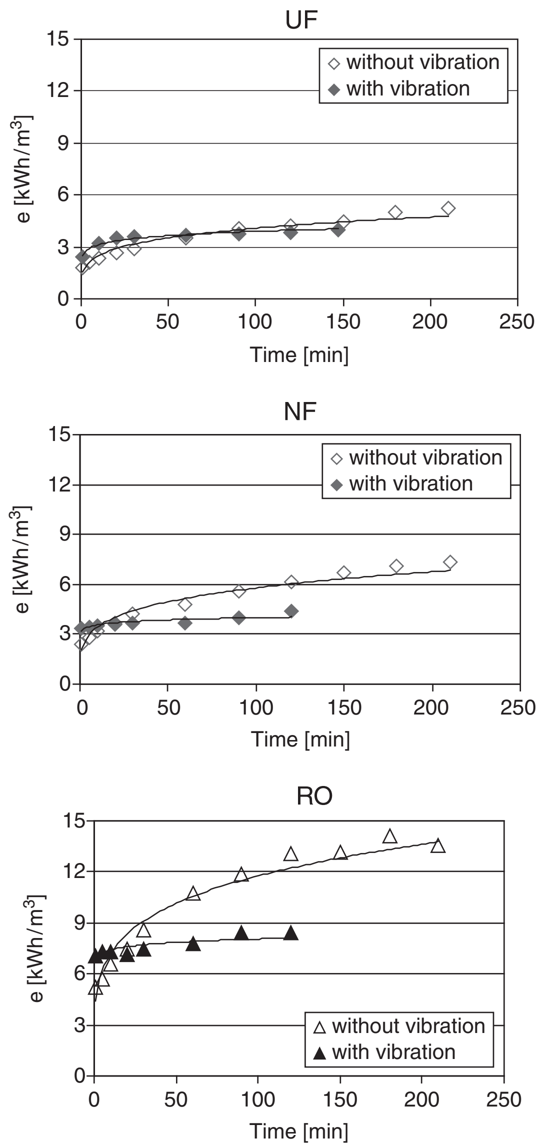

Fig. 9. Specific energy demand per m^3 permeate during concentration experiments.

The vibration increased the COD rejection in the case of UF, but only marginally affected the efficiency of NF and RO, since the original value of it was quite high.

The mean shear rates and specific energy demand were calculated and compared in all cases. At the beginning of the filtration (before the building of polarization layer on the surface of the membrane) the specific energy demand per m^3 permeate was lower at non-vibrating systems, but at the end of the concentration the vibration decreased the specific energy demand. The difference between the vibrating and non-vibrating methods is most expressed in the case of RO. During UF and NF at lower pressures, the energy consumption of vibratory systems is higher than without vibration; but over a pressure value the vibration become more economical. This type of critical pressure value was not observed during RO; the energy demand of vibration systems was higher at all TMP.

Acknowledgements

The authors are grateful for support of the work provided by the "Optimization of Cost Effective and Environmentally Friendly Procedures for Treatment of Regional Water Resource" IPA Cross-border cooperation program (Serbia-Hungary) HUSRB 0901 and additionally, Szabolcs Kertész acknowledge the financial support of the Deák Ferenc predoctoral Hungarian fellowship.

References

[1] A. Román, J. Wang, J. Csanádi, C. Hodúr and Gy. Vatai, Partial demineralization and concentration of acid whey by nanofiltration combined with diafiltration, Desalination, 241 (2009) 288–295.
[2] B. Koroknai, Zs. Csanádi, L. Gubicza and K. Bélafi-Bakó, Preservation of antioxidant capacity and flux enhancement in concentration of red fruit juices by membrane processes, Desalination, 228 (2008) 295–301.
[3] Z. Šereš, J. Gyura, M. Djurić, Gy. Vatai and A. Jokić, Separation of non-sucrose compounds from sugar-beet syrup by ultrafiltration with ceramic membrane containing static mixer, Desalination, 250 (2010) 136–143.
[4] Gy. Vatai, D.M. Krstic, W. Höflinger, A. Koris and M. Tekic, Combining air sparging and the use of a static mixer in cross-flow ultrafiltration of oil/water emulsion, Desalination, 204 (2007) 255–264.
[5] J. Zhong, X. Sun and C. Wang, Treatment of oily wastewater produced from refinery processes using flocculation and ceramic membrane filtration, Sep. Purif. Technol., 32 (2003) 93–98.
[6] B. Reed, W. Lin, R. Viadero Jr. and J. Young, Treatment of oily wastes using high-shear rotary ultrafiltration, J. Environ. Eng., 123(12) (1997) 1234–1242.
[7] O. Akoum, M.Y. Jaffrin, L.H. Ding and M. Frappart, Treatment of dairy process waters using a vibrating filtration system and NF and RO membranes, J. Membr. Sci., 235 (2004) 111–122.
[8] M. Frappart, O. Akoum, L.H. Ding and M. Y. Jaffrin, Treatment of dairy process waters modelled by diluted milk using dynamic nanofiltration with a rotating disk module, J. Membr. Sci., 282 (2006) 465–472.
[9] J. Lee, S. Kim, J. Choi, H. Hwang, M. Cha and J. Kim, Tertiary treatment of biologically treated piggery wastewater using vibratory shear-enhanced RO membrane, Water Sci. Technol., 49(5–6) (2004) 435–442.
[10] T. Huuhilo, P. Vaisanen, J. Nuortila-Jokinen and M. Nyström, Influence of shear on flux in membrane filtration of integrated pulp and paper mill circulation water, Desalination, 141(3) (2001) 245–258.
[11] Sz. Kertész, S. Beszédes, Zs. László, G. Szabó and C. Hodúr, Nanofiltration and reverse osmosis of pig manure: Comparison of results from vibratory and classical modules, Desalin. Water Treat., 14 (2010) 233–238.
[12] H.B. Winzeler and G. Belfort, Enhanced performance for pressure-driven membrane processes: the argument for fluid instabilities, J. Membr. Sci., 80 (1993) 35–47.
[13] O.A. Akoum, M.Y. Jaffrin, L. Ding, P. Paullier and C. Vanhoutte, An hydrodynamic investigation of microfiltration and ultrafiltration in a vibrating membrane module, J. Membr. Sci., 197 (2002) 37–52.
[14] M. Kazemimoghadam and T. Mohammadi, Chemical cleaning of ultrafiltration membranes in the milk industry, Desalination, 204 (2007) 213–218.